

RESEARCH PAPER



Meta-analysis of shotgun sequencing of gut microbiota in obese children with MASLD or MASH

Thomas Zöggeler^{a*}, Anna Maria Kavallar^{a*}, Adam Robert Pollio^{b*}, Denise Aldrian^a, Cornelia Decristoforo^a, Sabine Scholl-Bürgi^a, Thomas Müller^a, and Georg Friedrich Vogel^{a,b} 

^aDepartment of Paediatrics I, Medical University of Innsbruck, Innsbruck, Austria; ^bInstitute of Cell Biology, Medical University of Innsbruck, Innsbruck, Austria

ABSTRACT

Alterations in the gut microbiome affect the development and severity of metabolic dysfunction-associated steatotic liver disease (MASLD) or metabolic dysfunction-associated steatohepatitis (MASH). We analyzed microbiomes of obese children with and without MASLD, MASH, and healthy controls. Electronic databases were searched for studies on the gut microbiome in children with obesity with/without MASLD or MASH, providing shotgun-metagenomic-sequencing data. Nine studies and an additionally recruited cohort were included. Fecal microbiomes of children with MASLD ($n = 153$) and MASH ($n = 70$) were significantly different in alpha- and beta-diversity ($p < 0.001$) compared to obese ($n = 58$) and healthy ($n = 132$). Species *Faecalibacterium_prausnitzii* and *Prevotella_copri* are differentially abundant between obese, MASLD and MASH groups. XGBoost and random forest-models accurately predict MASLD over obesity with an AUROC of 87% and MASH over MASLD with 89%. Pathway-abundance-based models accurately predict MASLD over obesity with an AUROC of 81% and MASH over MASLD with 88%. The composition of the gut microbiome is altered with increasing hepatic fibrosis and concomitant species-abundance increase of *Prevotella_copri* ($p = 0.0082$). Machine-learning models discriminate pediatric from adult MASH with an AUROC of 97%. The gut microbial composition is increasingly altered in children with the progression of MASLD toward MASH. This can be utilized as a fecal biomarker and highlights the impact of diet on the gut microbiome for disease intervention.

ARTICLE HISTORY

Received 31 July 2024
Revised 25 March 2025
Accepted 14 May 2025

KEYWORDS



NAFLD; NASH; fibrosis;
shotgun metagenomics;
microbiome

Introduction


Metabolic dysfunction-associated steatotic liver disease (MASLD) is the most common cause of chronic liver disease in children and adolescents and, when progressing progress to steatohepatitis, cirrhosis and end-stage liver disease, the second most common reason for liver transplantation in the world for adults, as it might.^{1,2} Globally, the MASLD prevalence is estimated to range between 5% and 8%.³ It is defined as the pathological accumulation of lipid droplets in >5% of hepatocytes with at least one out of five cardiometabolic criteria, e.g., presence of impaired glucose regulation, type 2 diabetes, overweight or obesity, hypertension or dyslipidemia.^{4,5} It may develop into metabolic dysfunction associated steatohepatitis (MASH), characterized by hepatic inflammation and cell injury, which might further progress to

cirrhosis and end-stage liver disease.⁵ MASLD and MASH have recently emerged as the most prevalent chronic liver disorders in developed countries.^{6,7} Furthermore, patients with MASLD are at risk of type 2 diabetes mellitus, heart disease and, as a consequence of cirrhosis, liver cancer or other forms of malignancies.^{8,9} Although MASLD is a known complication of obesity in youth, factors contributing to disease severity and progression remain unknown.^{2,10}

The intestinal microbiome is a complex ecosystem composed of trillions of microbes, existing symbiotically with the host. The microbiome is semi-transitive impacted by both maternal and external factors. These compositional changes provide differentiating cues for immune development, mucosal protection, and metabolic functions.^{4,11} In

CONTACT Georg Friedrich Vogel  georg.vogel@i-med.ac.at  Department of Paediatrics I, Institute of Cell Biology, Medical University of Innsbruck, Anichstraße 35, 6020 Innsbruck, Austria

*Authors contributed equally.

 Supplemental data for this article can be accessed online at <https://doi.org/10.1080/19490976.2025.2508951>.

© 2025 The Author(s). Published with license by Taylor & Francis Group, LLC.

This is an Open Access article distributed under the terms of the Creative Commons Attribution-NonCommercial License (<http://creativecommons.org/licenses/by-nc/4.0/>), which permits unrestricted non-commercial use, distribution, and reproduction in any medium, provided the original work is properly cited. The terms on which this article has been published allow the posting of the Accepted Manuscript in a repository by the author(s) or with their consent.

some disorders describing the micro-ecology has given insights into overall disease development.¹² Growing evidence suggests that the composition of gut microbiota might predispose, even fuel the development of MASLD.^{6,13–15}

The characterization of the gut microbiota was driven by 16S-rRNA sequencing and deepened by improved accessibility to shotgun sequencing technologies.¹⁶ It has become evident that alterations in bacterial colonization result in changes of the dominant bacterial products in the gut, i.e. dietary metabolites, such as short-chain fatty acids (SCFA), trimethylamine N-oxide (TMAO) and secondary bile acids. These products function in many physiological traits of the epithelium, this includes facilitating the development of loosened epithelial tight junctions dubbed a “leaky gut”. Further, these weakened junctions lead to increased intestinal permeability and consecutively translocation of bacterial products, via the portal circulation, to the liver, potentially driving hepatic inflammation and concomitant parenchymal changes.^{14,17,18} These changes in gut microbiome composition can be both translated to diagnostic approaches as well as used to target and alter the gut microbiome by modifying agents such as dietary habits or pre- and probiotics. Our understanding of how these microbes and respective microbial metabolites influence inflammatory and other gut-related disorders is a steadily growing field.^{19–21}

Alterations in gut microbiome beta diversity were altered in both the MASLD and obese children as compared to the healthy control group.^{4,11} More specifically, a significant increase in Bacteroida and decrease in Firmicutes phyla were observed in MASLD children compared to healthy.²² Interestingly, these changes in gut microbiota can be observed early in infancy.²³ Which puts the influence of diet on the gut microbiome center stage for early dietary disease interventions. Furthermore, specific compositional changes of the intestinal microbiota were also shown to allow for MASH disease course prediction in adult cohorts.²⁴ A systematic approach to meta-analyze a larger pediatric cohort of the growing body of studies on gut microbial composition and metabolic function in patients with obesity and associated MASLD or MASH employing shotgun metagenomics is lacking. This study closes this gap

and further explores the applicability of recent machine learning algorithms in discriminating disease states in this large systematic cohort. The use of diverse cohorts of large datasets combined with modern machine learning tools should elucidate new avenues of understanding for the MASLD disease state.

Materials and methods

Ethics statement

This study was conducted in accordance with the guidelines of the Institutional Review Board of the Medical University of Innsbruck (nr. 1095/2020) and the Declaration of Helsinki and Istanbul. Written informed consent was obtained from participants included at the Medical University of Innsbruck.

Search strategy and data extraction

This systematic review was conducted in accordance with the Meta-analysis Of Observational Studies in Epidemiology (MOOSE) reporting guidelines.²⁵ Relevant studies to be included in the meta-analysis were identified by a systematic literature search using the following bibliographic databases: PubMed, Scopus and Web of Science, and NCBI, the Genome Sequence Archive (GSA) and the EMBL European nucleotide archive (ENA) as data repositories. Search terms are “pediatric”, “children”, “adolescence”, “childhood”, “infant”, “obesity”, “fatty liver”, “NAFLD”, “NASH”, “MASLD”, “MASH”, “steatosis”, “steatohepatitis”, “gut”, “microbiota”, “microbiome”, “shotgun” and “metagenomic”. For further details on the screening and extraction methodology see Supplementary Methods.

Inclusion and exclusion criteria

Studies on the gut microbiome in children with obesity with or without MASLD or MASH providing shotgun metagenomics sequencing data. Following the new diagnostic criteria for MASLD and pediatric recommendations,²⁶ patients formerly categorized as NAFLD with obesity and steatosis were subgrouped as

MASLD in this study. According to the findings of the European LITMUS consortium cohort, where 98% of patients diagnosed with NAFLD fulfilled the MASLD criteria.²⁷ MASLD diagnosis or exclusion must be based on ultrasound, magnetic resonance imaging or liver histology. A certain subset of adult studies will be included to allow comparison of gut microbial signatures between children/adolescents and adults with progressing MASLD and fibrosis. MASLD and MASH are used as terminology in this manuscript but given the recent changes in terminology, incorporated studies use NAFLD and NASH terminology.

Obesity was defined as a BMI in the 95th percentile or above, without MASLD subsequently referred to as subgroup “obese”. In addition, we excluded children without diagnosing markers such as, ultrasound, magnetic resonance imaging or liver histology. Studies that included type 2 diabetes patients were also excluded. MASLD diagnosis was based on ultrasound, liver histology or abdominal fast-magnetic resonance imaging to assess intrahepatic fat content. MASH was defined as an additional biochemical or biopsy proven hepatic inflammation.

Studies with insufficient raw data annotation, insufficient metadata, or without shotgun metagenomics sequencing data available (16S-rRNA sequencing) or use of antibiotics were excluded.

A local cohort was included fulfilling the above inclusion criteria after obtaining written consent to participate. Adult cohorts were selected based on the availability of raw sequencing and metadata to fit the ethnicities included in the pediatric cohort.

Shotgun metagenomic sequencing

Stool samples were collected and stored at -80°C . 250 mg of fecal sample were used to extract DNA with QIAmp PowerFecal Pro DNA kit (Qiagen, Venlo, The Netherlands). DNA was sent for library preparation and shotgun metagenomics sequencing using a DNBSEQ PE150 platform at BGI company (Shenzhen, China). For further details on raw sequencing read processing see Supplementary Methods.

Bioinformatics and statistical analyses

Taxonomic profiles and read counts were integrated into a phyloseq object using the R (R: A language and environment for statistical computing, R foundation for Statistical Computing, Vienna, Austria) package phyloseq for downstream analyses. The batch effect of the included studies was removed by applying MMUPHin with studies as batch effect and disease state as covariate.²⁸ Alpha-diversity was calculated based on richness (“observed”), and Shannon diversity measures and Mann-Whitney-U-tests were applied. Beta-diversity was visualized as principal coordinates analysis on the Bray-Curtis distance that is calculated after performing variance stabilizing transformation. Beta-diversity was tested using a non-parametric multivariate statistical permutation (permutational multivariate analysis of variance (PERMANOVA)) test with the R package vegan for differential taxa abundance, linear discriminant analysis effect size (LEfSe) (Kruskal and Wilcoxon-threshold ≤ 0.01 , LDA threshold ≥ 4) was used.

Random forest (RF) and Extreme Gradient Boosting (XGB), both with 10-fold cross validation and five repeats, were used to build prediction models for bacterial composition and metabolic pathways using the R package caret. RF hyperparameter tuning was carried out to define the ideal number of tries and trees. XGB hyperparameter tuning was carried out to define the ideal number of rounds, learning rate, maximum depth of a tree, gamma, minimum child weight, subsamples and column samples by tree. Here, we specifically took advantage of the shrinkage parameter to limit the overfitting of our XGB model. Receiver operating characteristics curves were plotted using the R package MLeval.

HUMANn3 output, e.g., metabolic pathway in MetaCyc nomenclature relative abundance as counts per million, was further analyzed for differential abundance after centered log ratio normalization by the ANOVA-like differential expression (ALDEx2) tool. Output was visualized as a volcano plot or bar chart using the R packages EnhancedVolcano and ggplot2.

Association analysis of taxonomic abundance on family level with sample metadata was done using

microbiome multivariable association with linear models (MaAsLin2). Fixed effects were ethnicity. A zero-inflated negative binomial regression with a taxa-prevalence-threshold of 0.1 was applied. The difference in taxonomic abundances was deemed significant when $p < 0.001$.

All statistical analyses were performed using R statistical software. Bonferroni-correction was applied to compensate for multiple testing and stated (BF) were used. A p -value ≤ 0.05 was considered significant. Samples with missing metadata were excluded from the according analysis. Bar, box and dot plots were generated via the R ggplot2 package, for dendrogram generation ggtree and ggtreeExtra were used and world map was generated using ggplot2 and maps. Schematics and figures were compiled using the Illustrator CC 2020 (Adobe).

Results

Study cohort

The study cohort comprises 353 individuals identified through a systematic literature and database search from nine studies^{4,7,10,11,29–33} (Figure 1a,b) and additional 60 individuals, who were recruited from our center. In total, the pediatric cohort comprises 281 individuals with obesity of which 153 with MASLD and 70 with MASH, and 132 healthy individuals as controls (Tables 1, 2). Median age of obese patients was 13 y (interquartile range (IQR) 9.6–14), 13 y (IQR 12–14.7, 62 not available (NA)) of patients with steatosis, 12 y (IQR 10–14) for individuals with MASH and 9 y (IQR 5.7–12) in the control group (Table 1). Median body mass index (BMI) was 30.2 (IQR 27.9–30.3) in obese patients, 31.1 (IQR 26.9–32.7) in MASLD patients and 30.8 (IQR 26.6–34.6) in patients with MASH and 16 (IQR 15.6–17.6) in the control group (Table 1). Median alanine aminotransferase (ALT) levels were 21 U/l (IQR 20.8–27) in obese, 48.6 U/l (IQR 30–57) in MASLD, and 63.1 U/l (IQR 31–60) in MASH, patients and 26 U/l (IQR 24.1–28.3) in the control group (Table 1). Median aspartate aminotransferase (AST) levels were 20.8 U/l (IQR 18.3–29) in obese, 40 U/l (IQR 32–40) in MASLD, and 40 U/l (IQR 32–57) in MASH, patients and 32 U/l (IQR 29.4–34.2) in the control

group (Table 1). In MASH patients, no or mild fibrosis (F0–1) was present in 48.6%, moderate fibrosis (F2) in 14.3% and severe (F3–4) in 8.6% of patients. Data on fibrosis was missing in 28.6%. An additional adult MASLD cohort with and without liver fibrosis comprising 163 individuals was included (Supplementary Table S1).^{27,34}

Composition of the gut microbiome

First, we assessed the ecological composition of gut microbiota. Observed richness was significantly reduced in patients with MASH compared to healthy (BF $p < 0.0001$), obese (BF $p < 0.0001$) and MASLD patients (BF $p = 0.0006$). We found no change in Shannon diversity between the different subgroups (Figure 1d). Further, microbial community composition of all groups (e.g., healthy, obese, MASLD and MASH) was different as tested by Bray-Curtis similarity (PERMANOVA all comparisons $p < 0.001$) (Figure 1e). We compared relevant relative change in abundance focusing on MASLD and MASH microbiome abundance both on phyla and on species. Bacteroidota was reduced in MASLD compared to healthy (BF $p < 0.0001$). In contrast, Firmicutes were increased in MASLD compared to healthy (BF $p = 0.00011$) (Figure 2a, Supplementary Figure S1A). We observed a difference in the relative abundance decrease of *Faecalibacterium prausnitzii* between obese and both MASLD ($p = 0.00059$) and MASH ($p = 0.00055$). We also saw a decrease in abundance in *Alistipes putredinis* between healthy and both MASLD ($p = 0.0033$), and MASH ($p = 0.0046$) (Figure 2b, Supplementary Figure S1B). Notably, *Eubacterium rectale* is comparatively more abundant in MASLD than in MASH (BF $p = 0.011$) and much more abundant in both MASLD and MASH compared to healthy ($p < 0.0005$, $p = 0.071$) (Figure 2b, Supplementary Figure S1B). As we could not observe a clear association of certain species with the analyzed conditions (Figure 2c), we further investigated organismal importance for differentiation in dichotomous disease states using linear discriminant (LEfSe) analysis. When comparing obese with MASLD patients, we found *Faecalibacterium prausnitzii* to be important for differentiation in the obese and *Hungatella hathewayi* in the MASLD group (Figure 2b,d). When

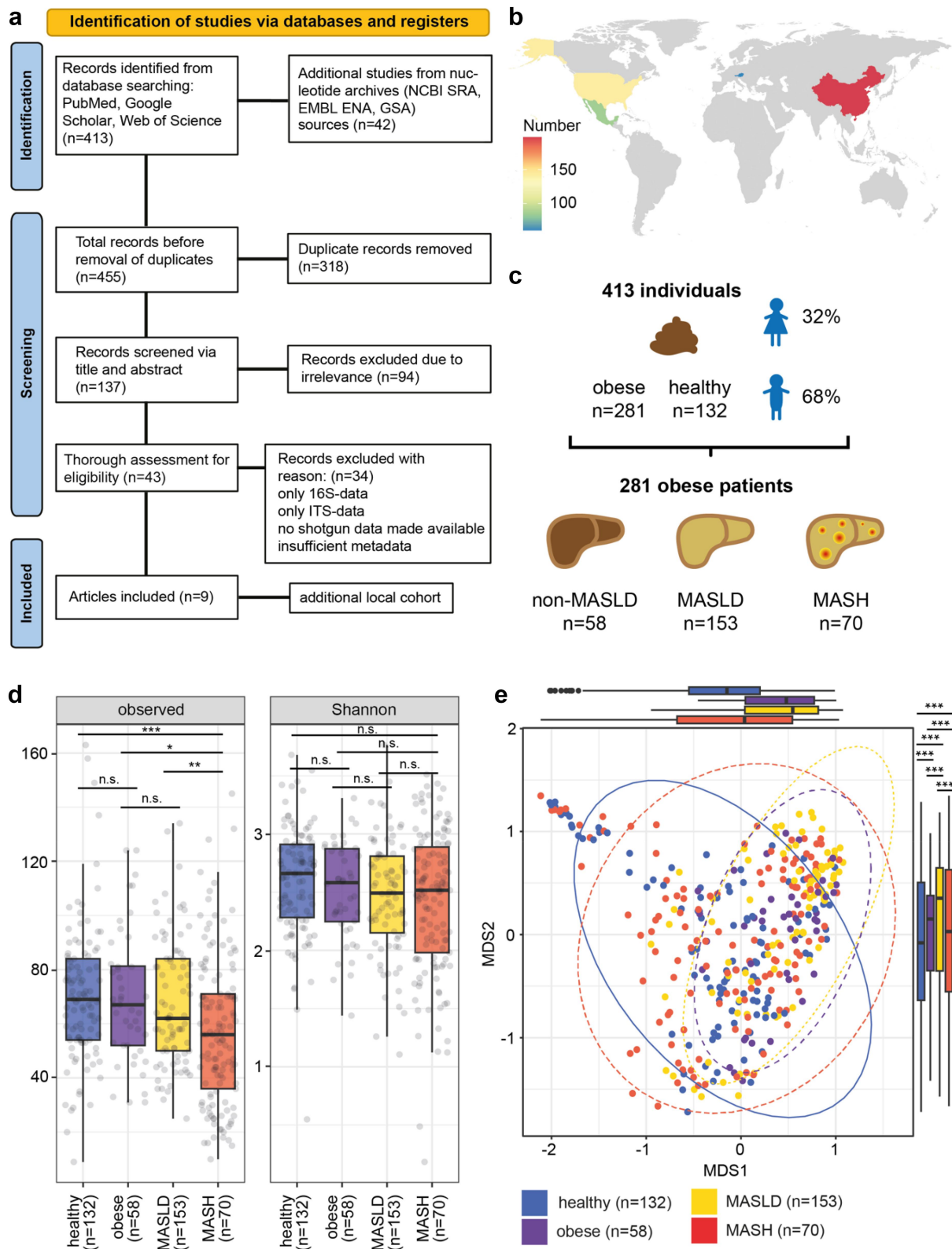


Figure 1. Study design, cohort composition and diversity metric: (a) meta-analysis of observational studies in epidemiology (MOOSE) flowchart depicting screening and selection process of studies included in the systematic review. (b) World map indicating countries of origin of patient cohort. (c) Schematic overview of the study cohort. (d) Alpha-diversity of gut microbiota shown as observed richness and Shannon diversity. In patients with MASLD and MASH in both richness (observed) and Shannon diversity metrics differed significantly; *** $p < 0.001$. Bonferroni corrected Mann–Whitney U tests were used. (E) Beta-diversity is shown as multidimensional scaling (MDS) using a principal coordinate analysis with Bray–Curtis distance measures. All groups differ markedly from each other; *** $p < 0.001$. PERMANOVA test was used.

Table 1. Composition of study cohort.

	Control (<i>n</i> = 132)	Obese (<i>n</i> = 58)	MASLD (<i>n</i> = 153)	MASH (<i>n</i> = 70)	p-value
Female (%)	60 (45.5), 5 NA	27 (46.6)	21 (31.8), 62 NA	17 (24.3)	$p < 0.001^*$
Median age in years (IQR)	9 (5.7–12)	13 (9.6–14)	13 (12–14.7), 62 NA	12 (10–14)	$p < 0.001^\ddagger$
Median BMI (IQR)	16 (15.6–17.6), 5 NA	30.2 (27.9–30.3)	31.1 (26.9–32.7)	30.8 (26.6–34.6)	$p < 0.001^\ddagger$
Median ALT U/l (IQR)	26 (24.1–28.3)	21 (20.8–27)	48.6(30–57)	63.1(31–60)	$p < 0.001^\ddagger$
Median AST U/l (IQR)	32 (29.4–34.2)	20.8 (18.3–29)	40.0 (32–40)	40(32–57)	$p < 0.001^\ddagger$
Hepatic fibrosis (%)					
0–1				34 (48.6%)	
2				10 (14.3)	
3				6 (8.6)	
NA				20 (28.6)	

ALT – alanine aminotransferase, AST – aspartate aminotransferase, BMI – body mass index, IQR – interquartile range, NA – not available; 4-group comparison p-values are calculated by * Fisher's exact test, ‡ Kruskal Wallis test.

Table 2. Included studies and characteristics of the individual study population and data availability.

Study	Cohort	Median age in years (IQR)	Median BMI (IQR)	City/country	Accession number
Kordy 2021	control (<i>n</i> = 20)	12 (8–14.3)	17.6 (15.9–18.9)	Los Angeles/USA	PRJNA480711
	MASH (<i>n</i> = 20)	12.5 (11–16)	32.7 (27.7–37)		
Li 2023	control (<i>n</i> = 22)	5.4 (5.2–6)	14.3 (13.5–14.8)	Chengdu/China	CNP0004872
Liang 2022	control (<i>n</i> = 5)	NA	NA	Beijing/China	CRA007303
	MASLD (<i>n</i> = 8)	NA	NA		
Maya-Lucas 2019	control (<i>n</i> = 10)	9.9 (9.9–9.9)	17.4 (17.4–17.4)	Mexico City/Mexico	PRJNA385215
Orbe-Orihuela 2022	control (<i>n</i> = 26)	9 (7–10)	16.4 (15.2–22.3)	NA/Mexico	PRJNA721692
Schwimmer 2019	MASLD (<i>n</i> = 38)	12.5 (11–13.8)	29.1 (26.3–32.8)	San Diego/USA	PRJNA546034
	MASH (<i>n</i> = 48)	12 (10–13.3)	29.9 (26–34.4)		
Testerman 2022	obese (<i>n</i> = 18)	12.6 (9.6–13.7)	30.3 (30.3–30.3)	New Haven/USA	PRJNA328258
	MASLD (<i>n</i> = 18)	12.9 (11.4–14.8)	35.2 (35.2–35.2)		
Zhang 2024	MASLD (62)	NA	NA	Beijing/China	PRJNA914785
Zhou 2022	control (<i>n</i> = 15)	13 (12–15.5)	20.7 (18.8–21.4)	Shenzen/China	PRJNA890867
	obese (<i>n</i> = 16)	14 (13–15)	28.4 (27.8–28.9)		
	MASLD (<i>n</i> = 27)	14 (12.5–16)	29.2 (28.1–32.4)		
This study	control (<i>n</i> = 34)	9 (7–12)	16 (15.1–18.4)	Innsbruck/Austria	PRJEB73820
	obese (<i>n</i> = 24)	10 (6–13)	29.2 (26.2–31)		
	MASH (<i>N</i> = 2)	12 (11.5–12.5)	34.8 (33.2–36.4)		

BMI–body mass index, IQR interquartile range, NA–not available.

MASH we compared to MASLD patients, *Dialister hominis* was a key marker in the MASH group (Figure 2e). We repeated this analysis on subgroups of our data to be sure that age nor gender were biasing our overall results. Thus, we compared subgroups of each population to see if there was any statistical variation (Supplementary Figure S2, 3 and 4). We found that there was a significant difference between the age subgroups for both patients with MASLD and obesity, but there were no obvious sources of differentiation in the overall dataset. Likewise, we saw a significant difference between the gender and the MASLD dataset, but also saw no overlapping markers of significance in the LDA (Supplementary Figure S2, 3 and 4).

Multivariable association analysis of overall taxonomic abundance and sample metadata further highlighted a positive association with *Klebsiella pneumonia* and *Phocaeicola plebius* with Chinese ethnicity and *Bacteroides nordii* with Hispanic ethnicity compared to Caucasian

ethnicity (Supplementary Figure S5A). It is of note that these associated microbes did not impact our comparison of patients with the disease of interest.

Gut microbial communities separate MASLD and MASH

As microbial community diversity differed particularly in patients with MASLD and MASH from healthy and obese groups, we focused further analysis on the composition of gut microbiota in pediatric patients with MASLD. While we found microbial richness and community structure to be altered between obese patients and MASLD patients ($p < 0.001$) (Figures 1e and 3a).

We trained supervised machine learning models to elucidate further any specific microbial compositional patterns that might better predict MASLD in patients as compared to the obese population. Using XGBoost, these microbial features had

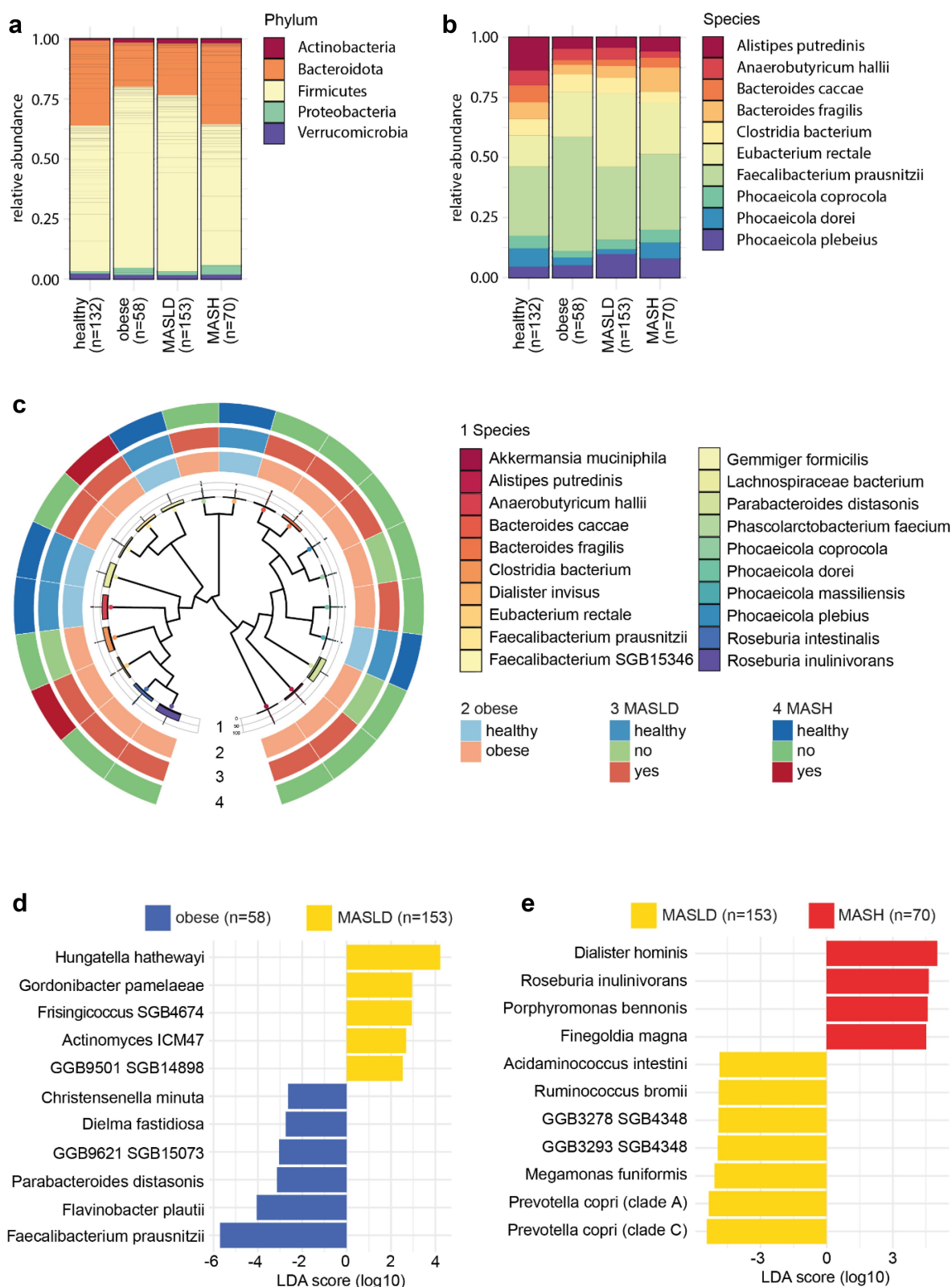


Figure 2. Relative abundance, disease association and differential abundance of taxa: (a) relative abundance of top 20 most abundant phyla is shown comparing healthy, obese, MASLD and MASH patients. Bacteroidota and firmicutes differ in abundance. (b) Relative abundance of top ten most abundant species is shown comparing healthy, obese, MASLD and MASH patients. (c) Dendrogram depicting top 20 most abundant species (inner circle/box plots) and associated conditions on the three outer circles. (d and e) linear discriminant analysis (LDA) showing differentially abundant species in (d) obese and MASLD patients and (e) in patients with MASLD or MASH.

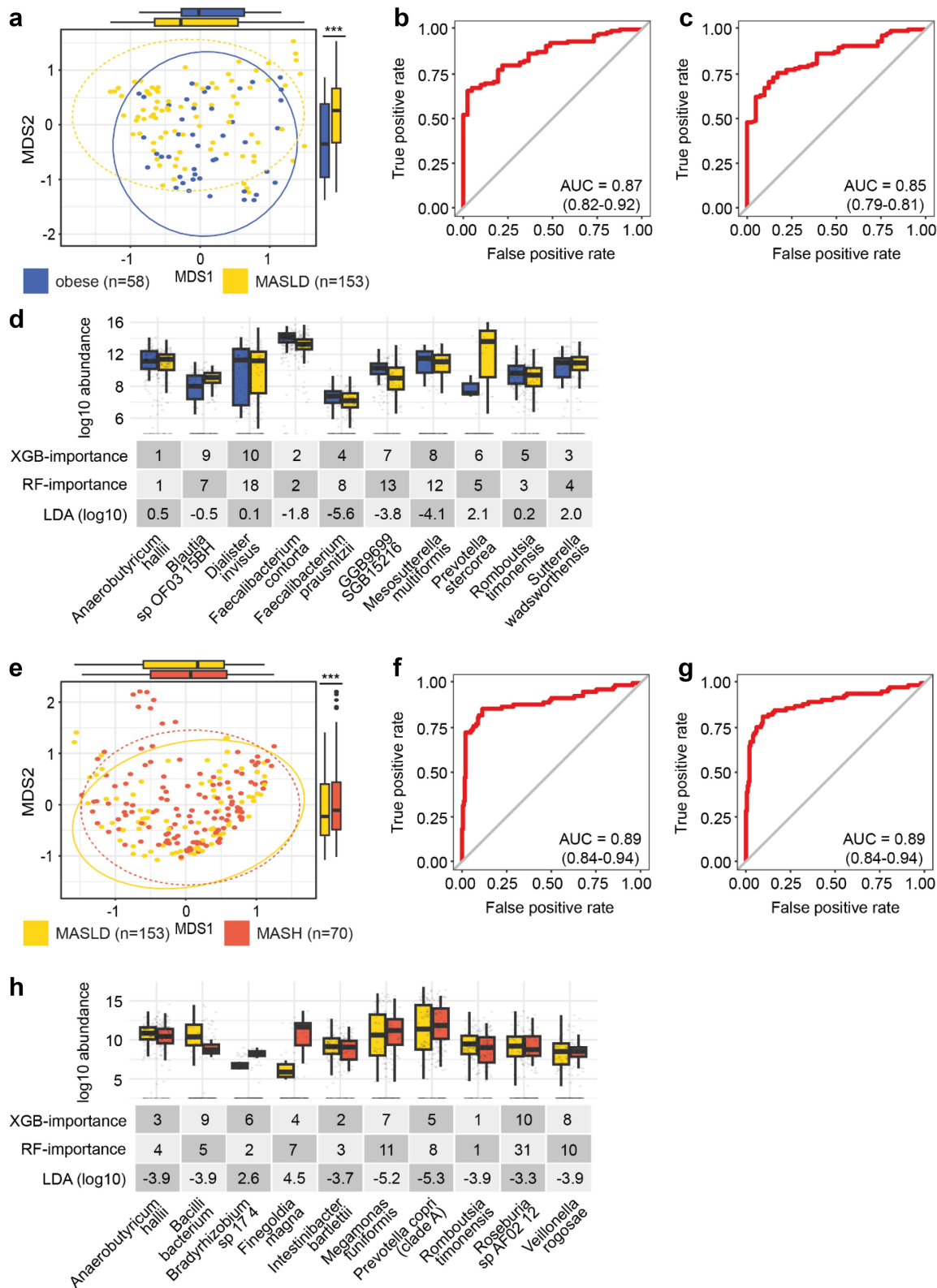


Figure 3. Community diversity and disease state prediction in MAFLD and MASH: (a) beta-diversity is shown as multidimensional scaling (MDS) using a principal coordinate analysis with Bray-Curtis distance measures. Both groups differ markedly from each other; *** $p < 0.001$. PERMANOVA test was used. (b) Area under the receiver operating characteristics curve (AUROC) of 83% (CI 0.79–0.87) of the XGBoost model discriminating obese patients with or without MASLD. (c) AUROC of 81% (CI 0.76–0.86) of the random forest model discriminating obese patients with or without MASLD. (d) Dotted box-plot of log10-transformed species abundance of top ten discriminative genus-features identified by supervised machine-learning with ranked feature importance of the XGBoost and random forest (RF) model, and LDA (log10) values from differential abundance analysis comparing obese patients with (yellow) against

a strong discriminatory power with an area under the receiver operating characteristic curve (AUROC) value of 87% (confidence interval (CI): 0.82–0.92) (Figure 3b, Supplementary Table S2). Applying a second model based on random forest reached an AUROC of 85% (CI: 0.79–0.81) (Figure 3c, Supplementary Table S3). Both models identified the abundance of *Anaeroburteicum hallii*, as the most distinguishing feature for differentiation (Figure 3d).

Using a similar methodology, we compared MASLD to MASH. Community structure was significantly different between patients with MASLD and MASH ($p < 0.001$), indicating an increasing interplay of the gut microbiome and progression of liver disease severity (Figures 1e and 3e). XGBoost and RF models were able to have strong discriminatory power of MASH over MASLD with an AUROC of 89% (CI: 0.84–0.94) (Figure 3f,g, Supplementary Table S4 and 5). Abundance of *Romboutsia timonensis*, *Intestinibacter bartlettii* and *Anaerobutyricum hallii* were among the top discriminative features of the model (Figure 3h).

In conclusion, the gut microbial composition is increasingly altered with the progression of MASLD toward MASH. This allows for accurate discrimination between pediatric MASLD and MASH.

Gut microbial metabolic pathways in pediatric MASLD

Taxonomic composition diverged between obese individuals and patients with MASLD, thus we studied the metabolic capacity of the metagenome. Differential abundance showed metabolic capabilities between the obese and MASLD patients changed but to a similarly minor degree as seen in the community-based analysis (Figure 4a). Conversely, comparisons between the MASLD and MASH groups revealed more significantly regulated pathways (Figure 4b, Supplementary Table S6 and 7).

When comparing MASLD patients to obese patients, no pathway was significantly changed ($\log_{10}(p) > 1.3$) (Figure 4a,c, Supplementary Table 6). In contrast, several pathways were significantly lower abundant in the MASLD patients ($\log_{10}(p) < -1.3$) (Figure 4a,c, Supplementary Table 6). The comparison between MASH and MASLD revealed several pathways that significantly changed in abundance. This illustrates the striking difference between the two microbial populations both in function and in composition (Figure 4b,d, Supplementary Table 7). Notably, nylon-6 oligomer degradation has a significantly higher abundance of gene abundance ($\log_{10}(p) < -3$) in the MASLD patients as compared to the MASH patients as well (Figure 4b,d, Supplementary Table 7). In order to further decipher the differences between groups, we trained XGBoost and RF models based on the abundance of metabolic pathway data with the intention of classifying MASLD and MASH, respectively, to the two comparisons of obese and MASLD. MASLD was distinguished with an AUCROC of 81% (CI: 0.76–0.86) by XGB and an AUCROC of 79% (0.73–0.85) in RF (Figure 4e and Supplementary Figure S6A). MASH was distinguished with an AUROC 88% (CI: 0.83–0.93, XGBoost) and an AUROC 85% (CI: 0.79–0.91, RF) (Figure 4f and Supplementary Figure S6C). Interestingly, the abundance of the “methanogenesis from acetate” pathway was the strongest discriminative feature to separate MASLD from both obesity and MASH by both models (Supplementary Figure S6B and D). This was further emphasized by the significant difference in abundance between MASLD and the other subgroups differential abundance analyses (Figure 4g).

In addition to this analysis, we specifically tested pathways previously reported for differential abundance in our groups. Lipopolysaccharides (LPS) and bacteria with flagellar gene complexes can

without (blue) MASLD. (e) Beta-diversity shown as MDS using a principal coordinate analysis with Bray-Curtis distance measures. Both groups differ markedly from each other; *** $p < 0.001$. PERMANOVA test was used. (f) AUROC of 89% (CI 0.84–0.94) of the XGBoost model discriminating MASLD from MASH patients. (g) AUROC of 89% (CI 0.84–0.94) of the random forest model discriminating MASLD from MASH patients. (h) Dotted box-plot of \log_{10} -transformed species abundance of top ten discriminative genus-features identified by supervised machine-learning with ranked feature importance of the XGBoost and random forest (RF) model, and LDA (\log_{10}) values from differential abundance analysis comparing MASLD (yellow) from MASH (red) patients.

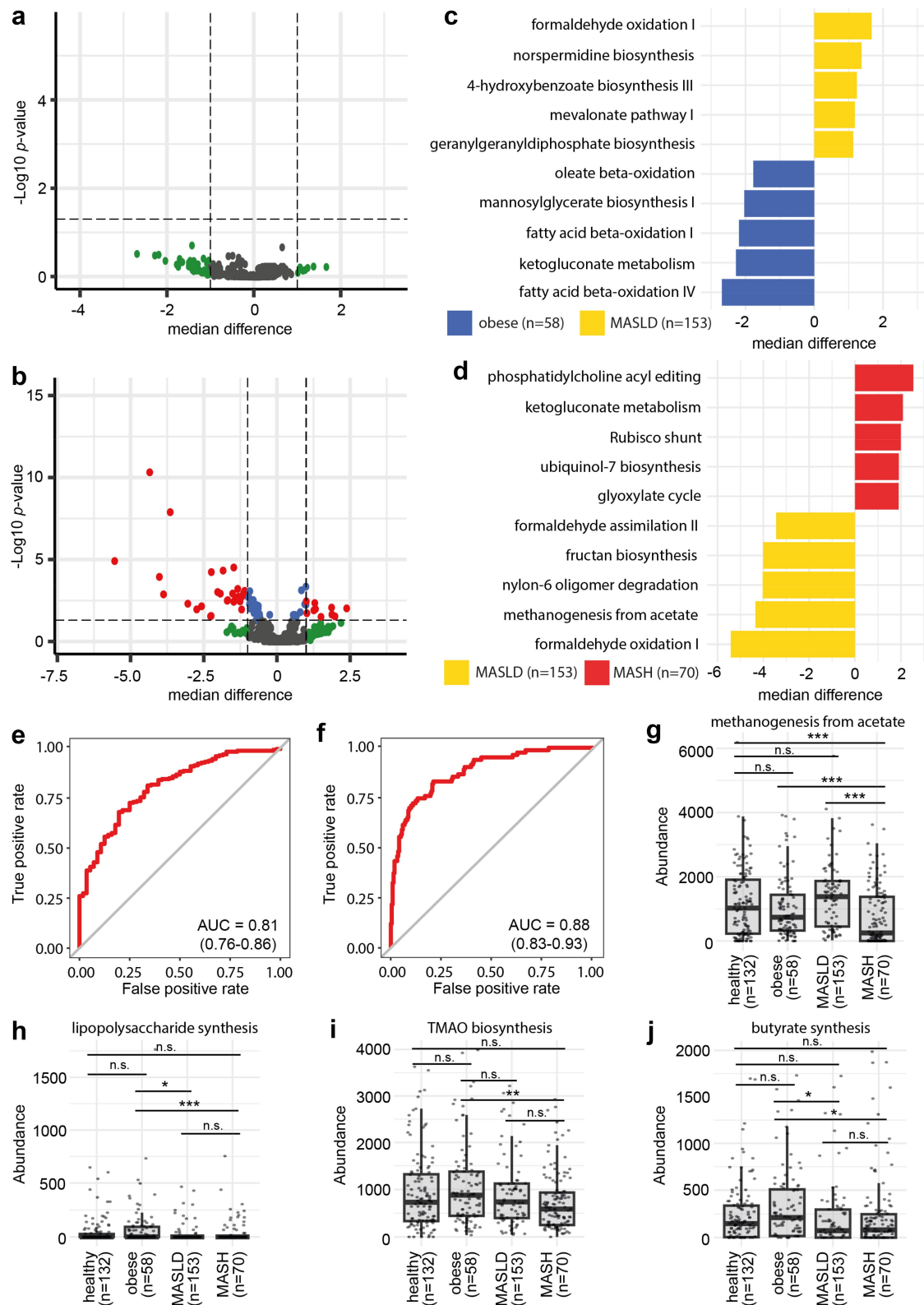


Figure 4. Microbial metabolic pathways: (a) volcano plot of differentially abundant pathways comparing obese (left) and MASLD patients (right). p-value cutoff is 0.05. (b) Volcano plot of differentially abundant pathways comparing MASLD (left) and MASH patients (right). p-value cutoff is 0.05. (c) Diverging bar charts of the top differentially abundant metabolic pathways from ALDEx2 analysis in obese and MASLD patients. (d) Diverging bar charts of the top differentially abundant metabolic pathways from ALDEx2 analysis in MASLD and MASH patients. (e) Area under the receiver operating characteristics curve (AUROC) of 80% (CI 0.75–0.85) of the XGBoost model discriminating MASLD based on metabolic pathway abundance. (f) AUROC of 88% (CI 0.83–0.93) of the XGBoost model discriminating MASH based on metabolic pathway abundance. (g) Dot-box-plot of the methanogenesis from acetate pathway-

trigger the immune system. LPS biosynthesis showed a decrease in abundance between both MASLD and MASH ($p = 0.042$, $p < 0.0001$) compared to the obese group (Figure 4h). Flagellar motility genes were not significantly altered by comparison of any group (Supplementary Figure S7A). Next, we studied SCFA biosynthesis. Abundance of butyrate synthesis was significantly decreased in both MASLD and MASH (BF $p = 0.031$ and 0.025) compared to the obese individuals (Figure 4j). In addition, we see this trend continues in propanoate production where MASLD and MASH are significantly decreased as compared to the obese group (Supplementary Figure 7B). Crucially, acetate production is significantly changed between the MASLD and MASH group with the MASLD population having an increase in abundance ($p = 0.0483$) (Supplementary Figure 7C). Finally, we found that secondary bile acid synthesis increased in MASH over MASLD individuals (BF $p = 0.046$) (Supplementary Figure 7D). TMAO biosynthesis was decreased in MASH ($p = 0.0078$) compared to obese individuals (Figure 4i).

Intestinal microbial ecology distinguishes fibrotic and adult MASLD

The gut microbiome is increasingly altered in patients with MASH. We further explored the effect of hepatic fibrosis on the microbiome. Again, we found microbial richness and community structure to be altered between different grades of MASH fibrosis (0–3) (0 vs. 2 BF $p < 0.032$, 1 vs. 2 BF $p = 0.04$, PERMANOVA all $p < 0.001$) but Shannon diversity was not altered ($p = 1$) (Figure 5a,b). The abundance of *Bifidobacterium adolescentis* (grade 0–1 vs. 3, BF $p = 0.027$ and $p = 0.028$) and *Prevotella copri* (clade A) (grade 0 vs. 2, BF $p = 0.0082$; grade 1 vs. 2, BF $p = 0.0091$) were altered between several of the grades (Supplementary Figure S8A).

We were further interested, whether pediatric/adolescent MASH affected the gut microbial

composition in a similar fashion as found in adult MASH patients. While richness was decreased between adult and pediatric MASH patients (BF $p < 0.001$), Shannon diversity was not different (Supplementary Figure 9A). Microbial community structure differed significantly between all four groups tested ($p < 0.001$), as well as more specifically between the pediatric and adult MASH groups with similar grade of fibrosis ($p < 0.001$) (Figure 5d, Supplementary Figure S9B). XGBoost and RF models distinguished pediatric from adult MASH with an AUROC of 97% (CI: 0.95–0.99, XGBoost) and an AUROC of 96% (CI: 0.93–0.99, RF) (Figure 5e,f, Supplementary Table S8 and 9). Abundance of *Prevotella copri* (clade A), *Romboutsia timonensis* and *Phocaeicola dorei* were among the top discriminative features of the model (Figure 5g). The composition of the gut microbiome is altered with increasing hepatic fibrosis and is clearly different between pediatric and adult MASH.

Discussion

Obesity, MASLD and MASH are on the rise globally, already affecting children and adolescents. Alterations in gut microbial composition are recognized not only as a consequence of altered systemic metabolism, but also as disease driving as gut and liver are in close concert anatomically, metabolically and immunologically. We have collected and systematically analyzed a large international pediatric cohort to study the gut microbiome with high sequencing resolution in obese patients with and without liver disease. We delineate these differences in microbial composition, which we feel can be utilized as biomarkers to predict the presence and stage of disease.

We observed changes in community structure and composition in gut microbiomes of obese patients with MASLD and MASH. Phylum-abundance of Bacteroidota was increased while Firmicutes were reduced in MASLD and MASH compared to obese children, consistent with prior

abundance. (h) Dot-box-plot of the lipopolysaccharide synthesis pathway-abundance. (i) Dot-box-plot of the trimethylamine N-oxide (TMAO) biosynthesis pathway-abundance. (j) Dot-box-plot of the butyrate synthesis pathway-abundance. (G–J): * $p < 0.05$, *** $p < 0.001$, n.s. not significant. Bonferroni corrected Mann–Whitney U tests were used.



Figure 5. Gut microbial dynamics in pediatric and adult patients with fibrosis: (a) alpha-diversity of gut microbiota differed in patients with MASH and grade 2 fibrosis in richness (observed). Shannon diversity metrics do not differ between groups; *** $p < 0.001$, n.S. not significant. Bonferroni corrected Mann–Whitney U tests were used. (b) Beta-diversity is shown as multidimensional scaling (MDS) using a principal coordinate analysis with Bray–Curtis distance measures. All groups differ markedly from each other; *** $p < 0.001$. PERMANOVA test was used. (c) Relative abundance of top 20 most abundant species is shown in patients with MASH and increasing grade of fibrosis. (d) Beta-diversity is shown as multidimensional scaling (MDS) using a principal coordinate analysis with Bray–Curtis distance measures. Colors indicate pediatric and adult MASH patients with symbols highlighting the grade of fibrosis. Both groups

findings.^{35,36} On a species-level, abundance dynamics of *Faecalibacterium prausnitzii* and *Alistipes putredinis* were found repetitively in differential abundance analyses. Our supervised machine learning models further showed the importance of *Faecalibacterium prausnitzii* microbial signatures to discriminate MASLD and MASH.

Altered abundance of *Faecalibacterium prausnitzii* is associated with various diseases. Specifically, reduced levels are seen in different intestinal disorders.³⁷ Supplementation with *Faecalibacterium prausnitzii* in mice improves metabolism, including enhanced glucose homeostasis, prevention of hepatic lipid accumulation, reduced liver damage and fibrosis, restoration of damaged gut barrier functions and alleviation of hepatic steatosis.³⁸ However, only limited data exist regarding changes in children. We found higher *Faecalibacterium prausnitzii* levels in overweight children than in those with MASLD and higher levels in MASLD than those with MASH. Our supervised machine-learning model could identify MASLD over obesity with high accuracy using *Faecalibacterium prausnitzii* as a key feature. Together, the reduced intestinal abundance of *Faecalibacterium prausnitzii* could serve as both a biomarker and a potential therapeutic target.

While we identified the abundance of *Prevotella copri* (clade A) as a discriminative feature with enrichment in MASH, it has also been found enriched in adult MASLD patients and linked to a higher risk of disease progression, possibly due to increased intestinal permeability and reduced butyrate production.³⁹ Genomic analysis revealed substantial functional diversity, particularly in carbohydrate metabolism, indicating that multi-generational dietary changes may contribute to reduced prevalence in westernized populations.

Our study further yields a comprehensive analysis of microbial metabolic pathway-abundance. While differential abundance testing and machine

learning models allow to separate MASLD and MASH from obesity based on gene and pathway-abundance, we have further studied specific metabolic pathways associated with MASLD and MASH pathophysiology. The SCFA butyrate and propionate were shown to be of benefit in MASLD and MASH as they attenuate immune response and thereby protect against hepatic inflammation.^{13,40} Indeed, we have found reduced pathway-abundance for butyrate and propionate-synthesis, as expressed among others in *Faecalibacterium prausnitzii* or *Prevotella spp.*,^{41,42} in MASLD and MASH. These results resemble known data in more general occurrence of MASLD.²⁰

The gut microbiome has a critical impact on bile acid homeostasis as it converts primary into secondary bile acids which are subsequently incorporated in the enterohepatic circulation. Alterations in bile acid levels and compositions have been reported in both MASLD and MASH.^{13,14,18} Indeed, our enzymatic-abundance analysis showed increased levels of bacterial bile acid synthesis in both obese and MASH patients. This has to be further validated by systemic and fecal bile acid measurements in larger cohorts and is of particular interest as modulation of the enterohepatic circulation by administration of farnesoid X receptor agonists are being tested in studies to treat MASH.⁴³

Interestingly, our data could not show a significant increase in pro-inflammatory bacterial stimuli, e.g., LPS or flagellar expression, as reported previously,⁴ which might be accounted to the larger samples size of our study. Furthermore, we could not find the endogenous bacterial ethanol production in the gut as was shown to be associated with MASLD and MASH.⁴² While this study was not based on biochemical measurements, we could not detect an increased expression of ethanol dehydrogenase. In this case, biochemical measurements are certainly the superior approach.

differ markedly from each other; *** $p < 0.001$. PERMANOVA test was used. (e) Area under the receiver operating characteristics curve (AUROC) of 97% (CI 0.95–0.99) of the XGBoost model discriminating pediatric from adult MASH patients. (f) AUROC of 96% (CI 0.93–0.99) of the random forest model discriminating pediatric from adult MASH patients. (g) Dotted box-plot of log10-transformed species abundance of top ten discriminative genus-features identified by supervised machine-learning with ranked feature importance of the XGBoost and random forest (RF) model, and LDA (log10) values from differential abundance analysis comparing pediatric (yellow) and adult (red) MASH patients.

We have further highlighted that gut microbial signatures of pediatric MASH patients differ from adult with comparable hepatic fibrosis grade. While a similar reduction in the beneficial species *Faecalibacterium prausnitzii* is found in progressed adult MASH, we do not find concomitant enrichment in *Veillonella* species, for example in our pediatric cohort.²⁴ Certainly, an important discriminator might be age and lifestyle. We therefore see utmost importance to focus on therapeutic approaches incorporating dietary changes and probiotics as children's gut microbiota maturation is heavily influenced by diet and lifestyle, with recent research showing adaptability to dietary changes until school age.⁴⁴ Our data corroborate this demand, as the lack of certain species in MASLD and MASH could be compensated by supplementation.

Moreover, the demonstrated differences in pediatric and adult microbiome in MASLD patients are corroborated by recent, partly meta-analytical, studies. While the presence of *Faecalibacterium* and *Roseburia* genera were associated with healthy controls in a study exploring the potential of a variety of supervised and advanced unsupervised ML algorithms comparing adult MASLD with alcoholic-associated liver disease, the microbiome patterns in diseased patients do not overlap with the pediatric pattern in our study.¹⁹ Recently, a study preprint was published highlighting the potential of integrating large-scale microbiome data with metabolite data from separate adult cohorts in combination with a sophisticated randomization approach, demonstrating an increase in *Parabacteroides* genera and the metabolite pregnenetriol sulfate in MASLD.⁴⁵ Interestingly, we do not observe similar relevance in our study, but comparable approaches are still lacking in pediatric cohorts.

Despite the inclusion of studies from various countries, the inclusion of shotgun sequencing data limits the number of studies. Moreover, we find a certain overrepresentation of Chinese and Hispanic ethnicities in our study cohort. As the composition of the gut microbiome is strongly influenced by dietary habits, the composition of our study cohort might of course impact on the results. By multivariable association analysis, we could identify several species positively associated with the ethnicities included in our study.

However, none of these species are among the key species identified in differential abundance analyses or machine-learning models applied for discrimination of MASLD or MASH.

Our study harbors several strengths, including a large sample size drawn from a multinational cohort, ensuring diverse representation. Additionally, applied sequencing techniques offer unparalleled resolution depth, allowing for comprehensive analysis. Moreover, we compare our findings with an adult cohort, providing valuable insights into age-related differences.

However, our study also has limitations, primarily stemming from its retrospective nature. While we analyze existing data together with our local cohort, inherent biases and missing information may influence our conclusions. Specifically in this analysis, we have inherent bias due to the populations we have sampled from. Our data has a high representation in specific regions across the world that add a layer of bias to all of our analysis. In addition, the lack of availability of natural cohorts of populations limited our ability to generate a validation cohort for the machine learning models. A validation cohort would not just allow us to test the viability of our conclusions but would spark further research that might elucidate specific biological implications of our findings. Despite these limitations, our study contributes to the understanding of the dynamics of gut microbiota in pediatric MASLD and MASH. Here, we both solidify some known bacteria that play a role in MASLD and MASH, as well as suggest new organism that might play a role in the future analysis. We were able to analyze microbiome data using machine learning approaches to better describe differences between the distinct disease states. Here, we give potential tools for clinicians and microbiologists to explore in new datasets the viability and importance of these microbial factors.

Acknowledgments

We would like to thank the investigators and participants in the "Intestinal Bacterial Metagenome in Pediatric Nonalcoholic Fatty Liver Disease" study. Access to the raw datasets was provided from dbGaP (dbGaP Study Accession: phs001837.v1.p1) after Medical University of Innsbruck IRB

approval. This manuscript was not prepared in collaboration with investigators of the “Intestinal Bacterial Metagenome in Pediatric Nonalcoholic Fatty Liver Disease” study and does not necessarily reflect the opinions or views of the consortium study, or the NIDDK.

Disclosure statement

No potential conflict of interest was reported by the author(s).

Funding

The work was supported by the Österreichische Gesellschaft für Kinder- und Jugendheilkunde.

ORCID

Georg Friedrich Vogel  <http://orcid.org/0000-0002-2515-4490>

Authors contributions

Thomas Zöggeler (Conceptualization: Equal; Data curation: Lead; Formal analysis: Equal; Methodology: Equal; Writing – original draft: Lead; Writing – review & editing: Equal)

Anna Maria Kavallar (Conceptualization: Equal; Data curation: Lead; Formal analysis: Equal; Methodology: Equal; Writing – original draft: Lead; Writing – review & editing: Equal)

Adam Pollio (Conceptualization: Supporting; Data curation: Supporting; Formal analysis: Equal; Writing – original draft: Equal; Writing – review & editing: Equal)

Denise Aldrian (Conceptualization: Supporting; Writing – review & editing: Equal)

Cornelia Decristoforo (Recruitment: Supporting; Writing – review & editing: Supporting)

Sabine Scholl-Bürgi (Conceptualization: Supporting; Writing – review & editing: Supporting)

Thomas Müller (Writing – review & editing: Supporting)

Georg-Friedrich Vogel (Conceptualization: Equal; Data curation: Supporting; Formal analysis: Equal; Project administration: Lead; Supervision: Lead; Visualization: Equal; Writing – original draft: Equal; Writing – review & editing: Equal)

Abbreviations

ALT	alanine aminotransferase
AST	aspartate aminotransferase
AUC	area under the curve
BF	Bonferroni correction
LDA	linear discriminant analysis
LEfSe	linear discriminant analysis effect size

MASLD	metabolic dysfunction associated steatotic liver disease
MASH	metabolic dysfunction association steatohepatitis
NAFLD	nonalcoholic fatty liver disease
NASH	nonalcoholic fatty steatohepatitis
BMI	body mass index
IQR	interquartile range
NA	not available
PERMANOVA	permutational multivariate analysis of variance
AUROC	area under the receiver operating characteristics curve
RF	random forest
SCFA	short-chain fatty acid
TMAO	trimethylamine N-oxide

Data transparency statement

Raw sequence files of the local cohort are available on the European Nucleotide Archive (ENA) accession PRJEB73820.

References

1. Younossi ZM, Zelber-Sagi S, Henry L, Gerber LH. Lifestyle interventions in nonalcoholic fatty liver disease. *Nat Rev Gastroenterol Hepatol.* 2023;20(11):708–722. doi: [10.1038/s41575-023-00800-4](https://doi.org/10.1038/s41575-023-00800-4).
2. Yu EL, Golshan S, Harlow KE, Angeles JE, Durelle J, Goyal NP, Newton KP, Sawh MC, Hooker J, Sy EZ, et al. Prevalence of nonalcoholic fatty liver disease in children with obesity. *J Pediatr.* 2019;207:64–70. doi: [10.1016/j.jpeds.2018.11.021](https://doi.org/10.1016/j.jpeds.2018.11.021).
3. Yu EL, Schwimmer JB. Epidemiology of pediatric non-alcoholic fatty liver disease. *Clin Liver Dis (Hoboken).* 2021;17(3):196–199. doi: [10.1002/cld.1027](https://doi.org/10.1002/cld.1027).
4. Schwimmer JB, Johnson JS, Angeles JE, Behling C, Belt PH, Borecki I, Bross C, Durelle J, Goyal NP, Hamilton G, et al. Microbiome signatures associated with steatohepatitis and moderate to severe fibrosis in children with nonalcoholic fatty liver disease. *Gastroenterology.* 2019;157(4):1109–1122. doi: [10.1053/j.gastro.2019.06.028](https://doi.org/10.1053/j.gastro.2019.06.028).
5. Rinella ME, Lazarus JV, Ratzliff V, Francque SM, Sanyal AJ, Kanwal F, Romero D, Abdelmalek MF, Anstee QM, Arab JP, et al. A multisociety delphi consensus statement on new fatty liver disease nomenclature. *J Hepatol.* 2023;79(6):1542–1556. doi: [10.1016/j.jhep.2023.06.003](https://doi.org/10.1016/j.jhep.2023.06.003).
6. Tilg H, Zmora N, Adolph TE, Elinav E. The intestinal microbiota fuelling metabolic inflammation. *Nat Rev Immunol.* 2020;20(1):40–54. doi: [10.1038/s41577-019-0198-4](https://doi.org/10.1038/s41577-019-0198-4).
7. Liang T, Li D, Zunong J, Li M, Amaerjiang N, Xiao H, Khattab NM, Vermund S, Hu Y. Interplay of

- lymphocytes with the intestinal microbiota in children with nonalcoholic fatty liver disease. *Nutrients*. 2022;14 (21):14. doi: [10.3390/nu14214641](https://doi.org/10.3390/nu14214641).
8. Targher G, Byrne CD, Tilg H. MASLD: a systemic metabolic disorder with cardiovascular and malignant complications. *Gut*. 2024;73:691–702. doi: [10.1136/gutjnl-2023-330595](https://doi.org/10.1136/gutjnl-2023-330595).
 9. Tacke F, Horn P, Wai-Sun Wong V, Ratzliff V, Bugianesi E, Francque S, Zelber-Sagi S, Valenti L, Roden M, Schick F, et al. EASL–EASD–EASO clinical practice guidelines on the management of metabolic dysfunction-associated steatotic liver disease (MASLD). *J Hepatol*. 2024;81(3):492–542. doi: [10.1016/j.jhep.2024.04.031](https://doi.org/10.1016/j.jhep.2024.04.031).
 10. Testerman T, Li Z, Galuppo B, Graf J, Santoro N. Insights from shotgun metagenomics into bacterial species and metabolic pathways associated with NAFLD in obese youth. *Hepatol Commun*. 2022;6(8):1962–1974. doi: [10.1002/hep4.1944](https://doi.org/10.1002/hep4.1944).
 11. Zhou J, Zhang Q, Zhao Y, Zou Y, Chen M, Zhou S, Wang Z. The relationship of megamonas species with nonalcoholic fatty liver disease in children and adolescents revealed by metagenomics of gut microbiota. *Sci Rep*. 2022;12(1):22001. doi: [10.1038/s41598-022-25140-2](https://doi.org/10.1038/s41598-022-25140-2).
 12. Hou K, Wu ZX, Chen XY, Wang JQ, Zhang D, Xiao C, Zhu D, Koya JB, Wei L, Li J, et al. Microbiota in health and diseases. *Signal Transduct Targeted Ther*. 2022;7 (1):135. doi: [10.1038/s41392-022-00974-4](https://doi.org/10.1038/s41392-022-00974-4).
 13. Fan Y, Pedersen O. Gut microbiota in human metabolic health and disease. *Nat Rev Microbiol*. 2021;19 (1):55–71. doi: [10.1038/s41579-020-0433-9](https://doi.org/10.1038/s41579-020-0433-9).
 14. Aron-Wisnewsky J, Vigliotti C, Witjes J, Le P, Holleboom AG, Verheij J, Nieuwdorp M, Clément K. Gut microbiota and human NAFLD: disentangling microbial signatures from metabolic disorders. *Nat Rev Gastroenterol Hepatol*. 2020;17(5):279–297. doi: [10.1038/s41575-020-0269-9](https://doi.org/10.1038/s41575-020-0269-9).
 15. Maher S, Rajapakse J, El-Omar E, Zekry A. Role of the gut microbiome in metabolic dysfunction-associated steatotic liver disease. *Semin Liver Dis*. 2024;44 (4):457–473. doi: [10.1055/a-2438-4383](https://doi.org/10.1055/a-2438-4383).
 16. Sharpton SR, Yong GJM, Terrault NA, Lynch SV. Gut microbial metabolism and nonalcoholic fatty liver disease. *Hepatol Commun*. 2019;3(1):29–43. doi: [10.1002/hep4.1284](https://doi.org/10.1002/hep4.1284).
 17. Salzman NH, Schwimmer JB. Pediatric nonalcoholic fatty liver disease and the microbiome: mechanisms contributing to pathogenesis and progression. *Curr Opin Endocr Metabolic Res*. 2021;19:22–29. doi: [10.1016/j.coemr.2021.05.003](https://doi.org/10.1016/j.coemr.2021.05.003).
 18. Kolodziejczyk AA, Zheng D, Shibolet O, Elinav E. The role of the microbiome in NAFLD and NASH. *EMBO Mol Med*. 2019;11(2):11. doi: [10.15252/emmm.201809302](https://doi.org/10.15252/emmm.201809302).
 19. Park IG, Yoon SJ, Won SM, Oh KK, Hyun JY, Suk KT, Lee U. Gut microbiota-based machine-learning signature for the diagnosis of alcohol-associated and metabolic dysfunction-associated steatotic liver disease. *Sci Rep*. 2024;14(1):16122. doi: [10.1038/s41598-024-60768-2](https://doi.org/10.1038/s41598-024-60768-2).
 20. Guo GJ, Yao F, Lu WP, Xu HM. Gut microbiome and metabolic-associated fatty liver disease: current status and potential applications. *World J Hepatol*. 2023;15 (7):867–882. doi: [10.4254/wjh.v15.i7.867](https://doi.org/10.4254/wjh.v15.i7.867).
 21. Keshet A, Segal E. Identification of gut microbiome features associated with host metabolic health in a large population-based cohort. *Nat Commun*. 2024;15(1):9358. doi: [10.1038/s41467-024-53832-y](https://doi.org/10.1038/s41467-024-53832-y).
 22. Zhu L, Baker SS, Gill C, Liu W, Alkhoury R, Baker RD, Gill SR. Characterization of gut microbiomes in non-alcoholic steatohepatitis (NASH) patients: a connection between endogenous alcohol and NASH. *Hepatology*. 2013;57(2):601–609. doi: [10.1002/hep.26093](https://doi.org/10.1002/hep.26093).
 23. Yong GJM, Porsche CE, Sitarik AR, Fujimura KE, McCauley K, Nguyen DT, Levin AM, Woodcroft KJ, Ownby DR, Rundle AG, et al. Precocious infant fecal microbiome promotes enterocyte barrier dysfunction, altered neuroendocrine signaling and associates with increased childhood obesity risk. *Gut Microbes*. 2024;16(1):2290661. doi: [10.1080/19490976.2023.2290661](https://doi.org/10.1080/19490976.2023.2290661).
 24. Oh TG, Kim SM, Caussy C, Fu T, Guo J, Bassirian S, Singh S, Madamba EV, Bettencourt R, Richards L, et al. A universal gut-microbiome-derived signature predicts cirrhosis. *Cell Metab*. 2020;32(5):878–888.e876. doi: [10.1016/j.cmet.2020.06.005](https://doi.org/10.1016/j.cmet.2020.06.005).
 25. Stroup DF, Berlin JA, Morton SC, Olkin I, Williamson GD, Rennie D, Moher D, Becker BJ, Sipe TA, Thacker SB. Meta-analysis of observational studies in epidemiology a proposal for reporting. *JAMA*. 2000;283(15):2008–2012. doi: [10.1001/jama.283.15.2008](https://doi.org/10.1001/jama.283.15.2008).
 26. Paediatric steatotic liver disease has unique characteristics: a multisociety statement endorsing the new nomenclature. *J Pediatr Gastroenterol Nutr*. 2024;78 (5):1190–1196. doi: [10.1002/jpn3.12156](https://doi.org/10.1002/jpn3.12156).
 27. Hardy T, Wonders K, Younes R, Aithal GP, Aller R, Allison M, Bedossa P, Betsou F, Boursier J, Brosnan MJ, et al. The European NAFLD registry: a real-world longitudinal cohort study of nonalcoholic fatty liver disease. *Contemp Clin Trials*. 2020;98:106175. doi: [10.1016/j.cct.2020.106175](https://doi.org/10.1016/j.cct.2020.106175).
 28. Ma S, Shungin D, Mallick H, Schirmer M, Nguyen LH, Kolde R, Franzosa E, Vlamakis H, Xavier R, Huttenhower C. Population structure discovery in meta-analyzed microbial communities and inflammatory bowel disease using MMUPHin. *Genome Biology*. 2022;23(1):208. doi: [10.1186/s13059-022-02753-4](https://doi.org/10.1186/s13059-022-02753-4).
 29. Maya-Lucas O, Murugesan S, Nirmalkar K, Alcaraz LD, Hoyo-Vadillo C, Pizano-Zarate ML, García-Mena J. The gut microbiome of Mexican children affected by obesity. *Anaerobe*. 2019;55:11–23. doi: [10.1016/j.anaerobe.2018.10.009](https://doi.org/10.1016/j.anaerobe.2018.10.009).
 30. Kordy K, Li F, Lee DJ, Kinchen JM, Jew MH, La Rocque ME, Zabih S, Saavedra M, Woodward C,

- Cunningham NJ, et al. Metabolomic predictors of non-alcoholic steatohepatitis and advanced fibrosis in children. *Front Microbiol.* **2021**;12:713234. doi: [10.3389/fmicb.2021.713234](https://doi.org/10.3389/fmicb.2021.713234).
31. Orbe-Orihuela YC, Godoy-Lozano EE, Lagunas-Martínez A, Castañeda-Márquez AC, Murga-Garrido S, Díaz-Benítez CE, Ochoa-Leyva A, Cornejo-Granados F, Cruz M, Estrada K, et al. Association of gut microbiota with dietary-dependent childhood obesity. *Arch Med Res.* **2022**;53(4):407–415. doi: [10.1016/j.arcmed.2022.03.007](https://doi.org/10.1016/j.arcmed.2022.03.007).
 32. Li P, Jiang J, Li Y, Lan Y, Yang F, Wang J, Xie Y, Xiong F, Wu J, Liu H, et al. Metagenomic analysis reveals distinct changes in the gut microbiome of obese Chinese children. *BMC Genomics.* **2023**;24(1):721. doi: [10.1186/s12864-023-09805-4](https://doi.org/10.1186/s12864-023-09805-4).
 33. Zhang J, Shi M, Zhao C, Liang G, Li C, Ge X, Pei C, Kong Y, Li D, Yang W, et al. Role of intestinal flora in the development of nonalcoholic fatty liver disease in children. *Microbiol Spectr.* **2024**;12(2):e0100623. doi: [10.1128/spectrum.01006-23](https://doi.org/10.1128/spectrum.01006-23).
 34. Loomba R, Seguritan V, Li W, Long T, Klitgord N, Bhatt A, Dulai PS, Caussy C, Bettencourt R, Highlander SK, et al. Gut microbiome-based metagenomic signature for non-invasive detection of advanced fibrosis in human nonalcoholic fatty liver disease. *Cell Metab.* **2019**;30(3):607. doi: [10.1016/j.cmet.2019.08.002](https://doi.org/10.1016/j.cmet.2019.08.002).
 35. Ridaura VK, Faith JJ, Rey FE, Cheng J, Duncan AE, Kau AL, Griffin NW, Lombard V, Henrissat B, Bain JR, et al. Gut microbiota from twins discordant for obesity modulate metabolism in mice. *Science.* **2013**;341(6150):1241214. doi: [10.1126/science.1241214](https://doi.org/10.1126/science.1241214).
 36. Yu Z, Yu XF, Zhao X, Su Z, Ren PG. Greater alteration of gut microbiota occurs in childhood obesity than in adulthood obesity. *Front Pediatr.* **2023**;11:1087401. doi: [10.3389/fped.2023.1087401](https://doi.org/10.3389/fped.2023.1087401).
 37. Leylabadlo HE, Ghotaslou R, Feizabadi MM, Farajnia S, Moaddab SY, Ganbarov K, Khodadadi E, Tanomand A, Sheykhsaran E, Yousefi B, et al. The critical role of faecalibacterium prausnitzii in human health: an overview. *Microb Pathog.* **2020**;149:104344. doi: [10.1016/j.micpath.2020.104344](https://doi.org/10.1016/j.micpath.2020.104344).
 38. Shin JH, Lee Y, Song EJ, Lee D, Jang SY, Byeon HR, Hong MG, Lee S-N, Kim H-J, Seo J-G, et al. Faecalibacterium prausnitzii prevents hepatic damage in a mouse model of NASH induced by a high-fructose high-fat diet. *Front Microbiol.* **2023**;14:1123547. doi: [10.3389/fmicb.2023.1123547](https://doi.org/10.3389/fmicb.2023.1123547).
 39. Moran-Ramos S, Cerqueda-García D, López-Contreras B, Larrieta-Carrasco E, Villamil-Ramírez H, Molina-Cruz S, Torres N, Sánchez-Tapia M, Hernández-Pando R, Aguilar-Salinas C, et al. A metagenomic study identifies a prevotella copri enriched microbial profile associated with non-alcoholic steatohepatitis in subjects with obesity. *J Gastro Hepatol.* **2023**;38(5):791–799. doi: [10.1111/jgh.16147](https://doi.org/10.1111/jgh.16147).
 40. Sarkar A, Mitra P, Lahiri A, Das T, Sarkar J, Paul S, Chakrabarti P. Butyrate limits inflammatory macrophage niche in NASH. *Cell Death Dis.* **2023**;14(5):332. doi: [10.1038/s41419-023-05853-6](https://doi.org/10.1038/s41419-023-05853-6).
 41. Fagundes RR, Bourgonje AR, Saeed A, Vich Vila A, Plomp N, Blokzijl T, Sadaghian Sadabad M, von Martels JZH, van Leeuwen SS, Weersma RK, et al. Inulin-grown faecalibacterium prausnitzii cross-feeds fructose to the human intestinal epithelium. *Gut Microbes.* **2021**;13(1):1993582. doi: [10.1080/19490976.2021.1993582](https://doi.org/10.1080/19490976.2021.1993582).
 42. Michail S, Lin M, Frey MR, Fanter R, Paliy O, Hilbush B, Reo NV. Altered gut microbial energy and metabolism in children with non-alcoholic fatty liver disease. *FEMS Microbiol Ecol.* **2015**;91(2):1–9. doi: [10.1093/femsec/fiu002](https://doi.org/10.1093/femsec/fiu002).
 43. Adorini L, Trauner M. FXR agonists in NASH treatment. *J Hepatol.* **2023**;79(5):1317–1331. doi: [10.1016/j.jhep.2023.07.034](https://doi.org/10.1016/j.jhep.2023.07.034).
 44. Derrien M, Alvarez AS, de Vos WM. The gut microbiota in the first decade of life. *Trends Microbiol.* **2019**;27(12):997–1010. doi: [10.1016/j.tim.2019.08.001](https://doi.org/10.1016/j.tim.2019.08.001).
 45. Yi X, Zhu H, He M, Zhong L, Gao S, Li M. **2024**. Identifying causal relations between gut microbiome, metabolic dysfunction-associated fatty liver disease and the novel mediators of blood metabolites. *bioRxiv* 2024:2024.2008.2005.606637.